

Electron capture and excitation in intermediate-energy He^{2+}-H(1s,2s) collisions

Yadong Liu(刘亚东), Congcong Jia(贾聪聪), Mingxuan Ma(马茗萱), Xiang Gao(高翔), Ling Liu(刘玲), Yong Wu(吴勇), Xiangjun Chen(陈向军), and Jianguo Wang(王建国)
Citation: Chin. Phys. B, 2024, 33 (**8**): 083401. DOI: 10.1088/1674-1056/ad5322

What follows is a list of articles you may be interested in

Theoretical investigation of electron-impact ionization of W^{8+} ion

Shiping Zhang(张世平), Fangjun Zhang(张芳军), Denghong Zhang(张登红), Xiaobin Ding(丁晓彬), Jun Jiang(蒋军), Luyou Xie(颉录有), Yulong Ma(马玉龙), Maijuan Li(李麦娟), Marek Sikorski, and Chenzhong Dong(董晨钟)
Chin. Phys. B, 2024, 33 (**3**): 033401. DOI: 10.1088/1674-1056/ad1487

Fragmentation dynamics of electron-impact double ionization of helium

Shiwei Liu(刘士炜), Difa Ye(叶地发), and Jie Liu(刘杰)
Chin. Phys. B, 2023, 32 (**6**): 063402. DOI: 10.1088/1674-1056/acbe33

Electron-impact ionization of W^{9+} and W^{10+}

Runjia Bao(鲍润家), Junkui Wei(魏军奎), Lei Chen(陈雷), Bowen Li(李博文), and Ximeng Chen(陈熙萌)
Chin. Phys. B, 2023, 32 (**6**): 063401. DOI: 10.1088/1674-1056/aca14d

Integral cross sections for electron impact excitations of argon and carbon dioxide

Shu-Xing Wang(汪书兴) and Lin-Fan Zhu(朱林繁)
Chin. Phys. B, 2022, 31 (**8**): 083401. DOI: 10.1088/1674-1056/ac6336

Electron-impact ionization cross section calculations for lithium-like ions

Guo-Jie Bian(卞国杰), Jyh-Ching Chang(张稚卿), Ke-Ning Huang(黄克宁), Chen-Sheng Wu(武晨晟), Yong-Jun Cheng(程勇军), Kai Wang(王凯), and Yong Wu(吴勇)
Chin. Phys. B, 2022, 31 (**1**): 013401. DOI: 10.1088/1674-1056/ac229e

---

DATA PAPER

Electron capture and excitation in intermediate-energy He^{2+}–H(1s,2s) collisions

Yadong Liu(刘亚东)[1,2], Congcong Jia(贾聪聪)[2], Mingxuan Ma(马茗萱)[2,3], Xiang Gao(高翔)[2], Ling Liu(刘玲)[2,†], Yong Wu(吴勇)[2,‡], Xiangjun Chen(陈向军)[1], and Jianguo Wang(王建国)[2]

[1] *Department of Modern Physics, University of Science and Technology of China, Hefei* 230026, *China*
[2] *Institute of Applied Physics and Computational Mathematitics, Beijing* 100088, *China*
[3] *Institute of Modern Physics, Key Laboratory of Nuclear Physics and Ion-Beam Application (MOE), Fudan University, Shanghai* 200433, *China*

(Received 24 April 2024; revised manuscript received 26 May 2024; accepted manuscript online 3 June 2024)

The semiclassical non-perturbative atomic orbital close-coupling approach has been employed to study the electron capture and excitation processes in He^{2+}–H(1s) and He^{2+}–H(2s) collision systems. In order to ensure the accuracy of our calculated cross sections, a large number of high excited states and pseudostates are included in the expansion basis sets which are centered on the target and projectile, respectively. The total and partial charge transfer and excitation cross sections are obtained for a wide-energy domain ranging from 1 keV/amu to 200 keV/amu. The present calculations are also compared with the results from other theoretical methods. These cross section data are useful for the investigation of astrophysics and laboratory plasma.

Keywords: atomic orbital close-coupling (AOCC) method, inelastic collision processes, electron capture and excitation

PACS: 34.50.Fa, 34.70.+e, 34.80.Dp **DOI:** 10.1088/1674-1056/ad5322

1. Introduction

The investigation of collisions between highly charged ions and atoms or molecules is very important in plasma physics and astrophysics. The scheme of neutral hydrogen beam injection heating plasma which is proposed by the ITER project in the magnetic confinement fusion experiment requires a large amount of cross section data about the atomic collision processes to model and diagnose fusion plasma.[1,2] In addition, most of the ions in the solar wind are proton and ionized helium.[3,4] When the solar wind ions collide with the neutral gas (H, He, CO) in comets or planetary atmosphere, electron capture and excitation processes will occur. The x-ray emission from the charge transfer processes can be used to identify the composition and abundance of the solar wind ions.[5–7] So the cross section data for He^{2+}–H(1s) collision system are useful for understanding and modeling the x-ray emission in the astrophysical environment. Some previous studies[3,4] have shown the existence of H(2s) excited state in the astrophysical environment, and therefore the cross section data involving He^{2+}–H(2s) system may also be important in astrophysics.

In this work, we have studied the electron capture and excitation processes in collisions of He^{2+} ions with H(1s, 2s) in the energy region of 1 keV/amu–200 keV/amu by employing the semiclassical atomic orbital close-coupling (AOCC) method. The inelastic collision processes between He^{2+} and H(1s) have been extensively studied in the past. Total single-electron-capture cross sections were measured by Bayfield *et al.*,[8] Olson *et al.*,[9] Shah *et al.*[10] and Hvelplund *et al.*[11] in the combined energy region of 1 keV/amu–500 keV/amu for this collision system. The partial cross sections for electron captured to He^{+}(2s) state were also obtained by Bayfield *et al.*[8] and Shah *et al.*[10] The partial excitation cross sections for H(2p), H(2s) and H(3p) formation were determined experimentally by Hughes *et al.*[12] and Detleffsen *et al.*[13] in the energy range of 10 keV/amu–300 keV/amu. On the theoretical side, the cross section calculations for He^{2+}–H(1s) system were performed by employing various methods to describe the collision dynamics. The AOCC method was used by Fritsch *et al.*,[14] Toshima *et al.*,[15] Liu *et al.*[16] and Agueny *et al.*[17] to study the charge transfer, excitation and ionization processes for this collision system in the combined energy region of 1 keV/amu–400 keV/amu with different sizes of expansion basis sets which are centered on the target and projectile, respectively. Fritsch *et al.*[14] used smaller Slater-type orbital (STO) basis sets to describe 22 atomic states of the target (H) and 38 atomic states of the projectile (He^{+}), respectively. Toshima *et al.*[15] selected 11s10p8d6f5g and 11s10p7d6f4g Gaussian-type orbital (GTO) basis sets for H and He^{+}. The STO basis sets employed by Liu *et al.*[16] included 174 orbitals centered on the target, covering all discrete states with $n \leq 6$ and 117 quasicontinuum states, and

†Corresponding author. E-mail: liu_ling@iapcm.ac.cn
‡Corresponding author. E-mail: wu_yong@iapcm.ac.cn

© 2024 Chinese Physical Society and IOP Publishing Ltd

20 orbitals centered on the projectile for all discrete states with $n \leq 4$. Agueny *et al.*[17] utilized two sets of GTO for the targets and projectiles, with their largest basis set being 16s13p10d7f4g. They obtained a more accurate cross-section by averaging the results from these two basis sets. Winter *et al.*[18] used the Sturmian-pseudostate close-coupling approach to calculate the total and partial cross sections for the electron capture, excitation and ionization processes for He^{2+}–H(1s) system in the energy region of 0.75 keV/amu–9.6 MeV/amu. Minami *et al.*[19] performed the calculations of charge transfer cross section for He^{2+}–H(1s) collision by using the classical trajectory Monte Carlo (CTMC), AOCC and lattice time-dependent Schrodinger equation (LTDSE) methods in 1 keV/amu–1000 keV/amu, respectively. Faulkner *et al.*[20] applied the wave-packet convergent close-coupling (WP-CCC) method to investigate the electron capture, excitation and ionization processes for this collision system in the energy region of 10 keV/amu–1000 keV/amu. For He^{2+}–H(2s) system, no experimental studies have been performed on the inelastic processes until now. On the theoretical side, the research mainly focused on the electron capture process. The molecular close-coupling (MOCC) method was employed by Blanco *et al.*[21] and Jouin *et al.*[22] to compute the total electron capture cross sections for this collision system in the combined energy region of 0.0625 keV/amu–9 keV/amu. The partial electron capture cross sections were calculated by Esry *et al.*[23] using the AOCC and CTMC methods in the energy region of 0.25 keV/amu–16 keV/amu. The total electron capture cross sections obtained with eikonal approximation were reported by Chan *et al.*[24] in the energy region of 10 keV/amu–500 keV/amu. The eikonal impulse approximation (EI), continuum-distorted-wave approximation (CDW) and first order Brinkman–Kramers approximation (BK1) were used by Montanari *et al.*[25] to study the total and partial capture cross sections for He^{2+}–H(2s) system in the energy region of 6.25 keV/amu–225 keV/amu. However, the investigations of the excitation process are very limited, except for the study of Agueny *et al.*[17]

The main motivation of the present work is to investigate the dynamics of electron capture and excitation processes in He^{2+}–H(1s, 2s) collision systems and provide the accurate the total and partial cross section data for the above two inelastic processes in a wide energy region. Therefore, we use larger basis sets in the current calculations than the previous AOCC method to ensure that the results are more accurate.

The paper is organized as follows. In Section 2, we briefly outline the AOCC method used in this work. Section 3 mainly presents and discusses the results of our calculations for He^{2+}–H(1s, 2s) collisions. Conclusions are given in Section 4. Atomic units are used throughout, unless explicitly indicated.

2. Theoretical method

The details of the AOCC method, employed in the present calculations, are given elsewhere.[26] Here we briefly outline the main features of the method. The motion of nuclei follows classical trajectories while the electronic dynamics is described with a quantum treatment in this method. The position vector of the projectile relative to the target is reasonably approximated by classical trajectories $\boldsymbol{R}(t) = \boldsymbol{b} + \boldsymbol{v}t$ (see Fig. 1), where $\boldsymbol{b}$ and $\boldsymbol{v}$ are the impact parameter and velocity, respectively. The asymptotic states of the target and projectile particles are described by Gaussian-type orbital (GTO) basis sets

$$\psi_{i(j)}^{\mathrm{T(P)}}(\boldsymbol{r}) = \sum_k c_k \chi_k(\boldsymbol{r}), \tag{1}$$

where

$$\chi_k(\boldsymbol{r}) = N_k x^{u_k} y^{v_k} z^{w_k} \mathrm{e}^{-\alpha_k r^2}. \tag{2}$$

The N_k is a normalization factor and u_k, v_k and w_k are integers ($k = 1, \ldots, N$). All possible combinations of u_k, v_k and w_k up to a given $l = u_k + v_k + w_k$ are employed to cover all spherical harmonics $Y_{l,m}$ for a given value of l.

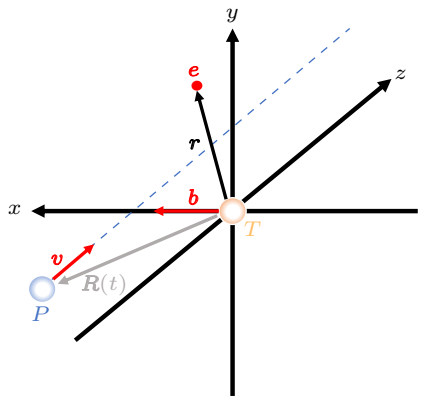


Fig. 1. Collision geometry. The impact parameter $\boldsymbol{b}$ and the projectile velocity $\boldsymbol{v}$ define the collision plane. The position of the electron with respect to the target center is denoted $\boldsymbol{r}$.

The total wavefunction of the collision system can be written as

$$\begin{aligned}\Psi(\boldsymbol{r}, \boldsymbol{R}(t)) = & \sum_i C_i^{\mathrm{T}}(t)\, \psi_i^{\mathrm{T}}(\boldsymbol{r})\, \mathrm{e}^{-\mathrm{i}\varepsilon_i^{\mathrm{T}} t} \\ & + \sum_j C_j^{\mathrm{P}}(t)\, \psi_j^{\mathrm{P}}(\boldsymbol{r})\, \mathrm{e}^{-\mathrm{i}\varepsilon_j^{\mathrm{P}} t}\, \mathrm{e}^{-\frac{\mathrm{i}}{2}v^2 t + \mathrm{i}\boldsymbol{v}\cdot\boldsymbol{r}},\end{aligned} \tag{3}$$

where ψ_i^{T} (ψ_j^{P}) and $\varepsilon_i^{\mathrm{T}}$ ($\varepsilon_j^{\mathrm{P}}$) are the atomic states and energies of the target and projectile, respectively. The states centered on projectile contain the plane-wave electron translation factor (ETF) $\mathrm{e}^{-\frac{\mathrm{i}}{2}v^2 t + \mathrm{i}\boldsymbol{v}\cdot\boldsymbol{r}}$, ensuring the Galilean invariance of the results.

The time-dependent Schrödinger equation of the active electron can be written as

$$\left[H - \mathrm{i}\frac{\partial}{\partial t}\right] \Psi(\boldsymbol{r}, \boldsymbol{R}(t)) = 0, \tag{4}$$

with the electronic Hamiltonian

$$\hat{H} = -\frac{1}{2}\nabla^2 + V_{\mathrm{T}} + V_{\mathrm{P}}, \tag{5}$$

where V_{T} and V_{P} are the interactions between the active electron and two nuclei, respectively, which are described by Coulomb potentials. Inserting the total wave function Eq. (3) into Schrödinger Eq. (4) leads to the first-order coupled differential equation for the scattering amplitude as

$$\mathrm{i}\frac{\mathrm{d}}{\mathrm{d}t}\boldsymbol{c}(t)=\boldsymbol{S}^{-1}(\boldsymbol{b},\boldsymbol{v},t)\,\boldsymbol{M}(\boldsymbol{b},\boldsymbol{v},t)\,\boldsymbol{c}(t), \tag{6}$$

where $\boldsymbol{c}$ is the column vector of the coefficients, $\boldsymbol{S}$ and $\boldsymbol{M}$ are the overlap and the coupling matrices, respectively.

The predictor–corrector method is used to solve the above first-order coupled differential equation to obtain the transition probability for an impact parameter and velocity as

$$P_{fi}(b,v_{\mathrm{p}})=\left|c_{fi}(b,t)\right|^2. \tag{7}$$

For a transition from an initial state to the final state $i\to f$, the cross section can be calculated as

$$\sigma_{fi}(v_{\mathrm{p}})=2\pi\int_0^{+\infty}bP_{fi}(b,v_{\mathrm{p}})\,\mathrm{d}b. \tag{8}$$

In our calculations, three basis sets (B1: 17s14p11d8f5g; B2: 18s15p12d9f6g; B3: 19s16p13d10f7g) are used for the H and He^+ centers in order to ensure better convergence of the results. The basis sets of the target (H) are given in Table 1. For the projectile, the GTO exponents can be deduced from H center by using the scaling law $\alpha_Z=\alpha_{\mathrm{H}}Z^2$.[27] All the basis sets include orbitals up to $n=5$ ($l=4$) for both target and projectile. The binding energies of H atoms and He^+ ions which are calculated by the above basis sets are provided in Table 2 and compared with the corresponding data from NIST.[28] The overall agreement between our calculations and NIST data[28] is very good and the relative differences are less than 0.06%.

Table 1. The GTO exponents (α_n) of hydrogen atom. The values of β for each l follow a geometric sequence according to $\alpha_n=\alpha\beta^{1-n}$, and n is the number of GTO.

	B1			B2			B3		
l	α	β	n	α	β	n	α	β	n
s	100	1.3335	17	100	1.3111	18	100	1.2915	19
p	10	1.425	14	10	1.3894	15	10	1.3593	16
d	1	1.584	11	1	1.5199	12	1	1.4677	13
f	0.1	1.93	8	0.1	1.7783	9	0.1	1.6681	10
g	0.01	1.775	5	0.01	1.585	6	0.01	1.4677	7

Table 2. Comparison of binding energies (E; in a.u.) of H atom and He^+ ion with the NIST[28] data.

	State	E_{ref}	E(B1)	Δ^*	E(B2)	Δ^*	E(B3)	Δ^*
H	1s	−0.4997333	−0.4999920	0.052%	−0.4999956	0.052%	−0.4999913	0.052%
	2s	−0.1249339	−0.1249990	0.052%	−0.1249994	0.052%	−0.1249989	0.052%
	2p	−0.1249329	−0.1250000	0.054%	−0.1250000	0.054%	−0.1250000	0.054%
	3s	−0.0555260	−0.0555552	0.053%	−0.0555554	0.053%	−0.0555552	0.053%
	3p	−0.0555257	−0.0555554	0.053%	−0.0555555	0.054%	−0.0555555	0.054%
	3d	−0.0555255	−0.0555555	0.054%	−0.0555556	0.054%	−0.0555556	0.054%
	4s	−0.0312333	−0.0312497	0.053%	−0.0312499	0.053%	−0.0312499	0.053%
	4p	−0.0312332	−0.0312494	0.052%	−0.0312500	0.054%	−0.0312500	0.054%
	4d	−0.0312331	−0.0312500	0.054%	−0.0312500	0.054%	−0.0312500	0.054%
	4f	−0.0312330	−0.0312499	0.054%	−0.0312499	0.054%	−0.0312499	0.054%
He^+	1s	−1.9998160	−1.9999661	0.008%	−1.9999558	0.007%	−2.0000130	0.010%
	2s	−0.4999626	−0.4999958	0.007%	−0.4999946	0.006%	−0.5000014	0.008%
	2p	−0.4999470	−0.4999998	0.011%	−0.4999999	0.011%	−0.4999999	0.011%
	3s	−0.2222030	−0.2222208	0.008%	−0.2222206	0.008%	−0.2222226	0.009%
	3p	−0.2221983	−0.2222217	0.011%	−0.2222222	0.011%	−0.2222222	0.011%
	3d	−0.2221941	−0.2222221	0.013%	−0.2222222	0.013%	−0.2222222	0.013%
	4s	−0.1249880	−0.1249989	0.009%	−0.1249993	0.009%	−0.1250002	0.010%
	4p	−0.1249861	−0.1249975	0.009%	−0.1249998	0.011%	−0.1250000	0.011%
	4d	−0.1249843	−0.1249999	0.012%	−0.1250000	0.013%	−0.1250000	0.013%
	4f	−0.1249835	−0.1249995	0.013%	−0.1249997	0.013%	−0.1249998	0.013%

$^*\Delta=\left|E_{\mathrm{present}}-E_{\mathrm{Nist}}\right|/E_{\mathrm{Nist}}$.

3. Results and discussion

In order to obtain better convergent cross sections, a large number of bound states and some pseudostates are included in the expansion basis sets on two centers to fully take into account the effect of multichannel couplings in the present calculations. We use three sets of GTOs which are shown in Table 1 to calculate the cross sections. The B1, B2 and B3 basis sets are composed of 215 GTOs, 240 GTOs and 265 GTOs, respectively. Almost all pseudostates (200–300) generated by each Gaussian basis of He^+ and H centers are included in the coupling calculation with a total of 554, 624 and 693 reaction channels, respectively. The GTOs are square-integrable L^2 functions and cannot describe the exact boundary conditions of continuum states.[29] In order to reduce the error of GTOs in describing pseudostates, the present cross sections can be given by the average values of the cross sections which

are obtained with the above three basis sets as

$$\sigma_{\text{Present}} = \frac{1}{3} \times (\sigma_{\text{B1}} + \sigma_{\text{B2}} + \sigma_{\text{B3}}). \tag{9}$$

3.1. He^{2+}–H(1s) collision

3.1.1. Excitation cross sections

The cross sections for excitation to $2l$, $3l$, $n = 4$ and $n = 5$ states of H atoms in He^{2+}–H(1s) system are given in Figs. 2(a)–2(f), respectively. The results of the present AOCC method are compared with the previous AOCC calculations by Toshima *et al.*,[15] Fritsch *et al.*,[14] Agueny *et al.*,[17] Liu *et al.*,[16] WP-CCC calculations of Faulkner *et al.*,[20] and with the calculations of the coupled-Sturmain approach of Winter *et al.*[18] In the same figure, the experimental data of 2l and 3p states from Hughes *et al.*[12] and Detleffsen *et al.*[13] are also shown. It can be seen from Figs. 2(a), 2(b) and 2(d) that the differences between the experimental data and most of the theoretical results are obvious. For cross sections of excitation to the 2s and 2p states, the experiment data of Hughes *et al.*[12] overestimate most of the theoretical results, except for the 30 keV/amu–40 keV/amu for the 2s state and 30 keV/amu–60 keV/amu for the 2p state, respectively. However, the experimental data from Detleffson *et al.*[13] are in general agreement with most of the theoretical calculations, including our AOCC results, for the energy region above 80 keV/amu. These discrepancies between experimental data and theoretical results may be from the fact that the hydrogen atomic targets in these experiments[12,13] were produced by using the highly dissociated hydrogen molecule beam, leading to a mixture of hydrogen molecule in the target. By comparing our results with other theoretical results in Figs. 2(a)–2(f), we can see that our results are consistent with the trend of the new results of Liu *et al.*,[16] Faulkner *et al.*[20] and Agueny *et al.*[17] However, the cross sections for excitation to 2s, 3s, and 3d states have certain gaps near the peak in Figs. 2(a), 2(c), 2(e). The differences are mainly due to the different types and sizes of the expansion basis sets centered on both target and projectile.

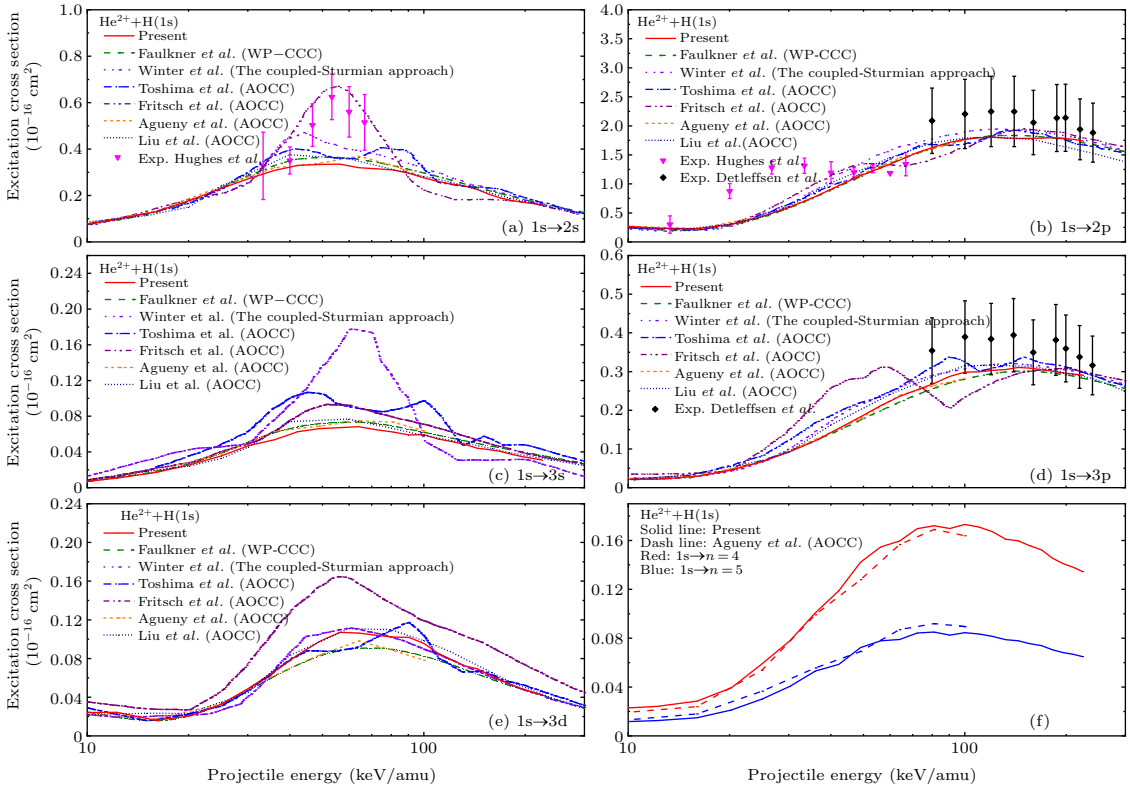


Fig. 2. The cross sections for excitation to $2l$, $3l$ states and $n = 4$, 5 shells of H atoms in He^{2+}–H(1s) collision. Theory: (solid red line) present results; (dashed olive line) WP-CCC results of Faulkner *et al.*;[20] (dotted violet line) coupled-Sturmain approach results of Winter *et al.*;[18] (dash-dotted blue line) AOCC results of Toshima *et al.*;[15] (dash-dot-dotted purple line) AOCC results of Fritsch *et al.*;[14] (short dashed orange line) AOCC results of Agueny *et al.*;[17] (short dotted royal line) AOCC results of Liu *et al.*[16] Experiment: (magenta triangles) Hughes *et al.*;[12] (black diamonds) Detleffsen *et al.*[13]

3.1.2. Electron capture cross sections

For the electron capture process, we summarize the theoretical and experimental results of the total electron capture cross sections in Fig. 3. It can be seen that our calculations are in good agreement with the experimental data[9–11] and other theoretical results[15,16,18,20] in the considered energy region, except for the experimental data of Bayfield *et al.*[8] It is obvious that the date from Bayfield *et al.*[8] are also larger than the other experimental[9,10] and theoretical data[15,16,18,20] in the energy region below about 40 keV/amu.

The partial cross sections for electron captured to the 1s, $2l$ and $3l$ states of He^+ ions are given in Fig. 4. For this col-

lision system, $n = 2$ is the dominant reaction channel. Only the cross section for electron captured to the 2s state has experimental values.[8,10] From Fig. 4(b), we can see that our results are in good agreement with other theoretical results[15–20] in the entire energy region. At the same time, the theoretical results in the 20 keV/amu–50 keV/amu energy range agree well with the experimental data of Shah *et al.*[10] For the results of capture to He^+(2p) state, no experimental data have been published to date. All the theoretical results have the same energy behavior in the considered energy region, but the magnitudes have slight differences. The present result is in the middle of two groups of theoretical results for collision energies below 100 keV/amu. When the collision energy is higher than 100 keV/amu, our result is in good agreement with the results of Toshima *et al.*,[15] Winter *et al.*,[18] Minami *et al.*[19] and Faulkner *et al.*[20] For the capture to the 1s state (Fig. 4(a)), all the theoretical cross sections reach the maximum value near the collision energy of 45 keV/amu. At higher energies, our results are a little larger than the other results. For the cross sections of capture to the 3*l* states (shown in Figs. 4(d)–4(f)), there is good agreement between different theoretical results[15,17–20] within the full energy range. In addition, we also provide the cross sections for electron captured to the $n = 1$–5 shells of H atoms in Fig. 5. The previous AOCC results of Agueny *et al.*[17] are also given for comparison. We can see that for the energies above 40 keV/amu, the 1s state of He^+ ion gradually becomes the dominant reaction channel for this collision system. When the collision energy is below 100 keV/amu, the present capture cross section of 2p state is lower than that of Agueny's (which is shown in Fig. 4(c)). This leads to a difference in the cross section of $n = 2$ channel.

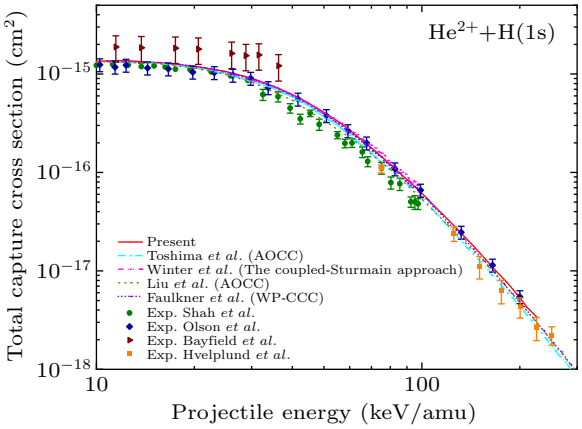


Fig. 3. The total electron capture cross sections as a function of energy in He^{2+}–H(1s) collision. Theory: (solid red line) present results; (dash-dotted cyan line) AOCC results of Toshima *et al.*;[15] (dash-dot-dotted magenta line) coupled-Sturmain approach results of Winter *et al.*;[18] (short dashed dark yellow line) AOCC results of Liu *et al.*;[16] (short dotted violet line) WP-CCC results of Faulkner *et al.*[20] Experiment: (green circles) Shah *et al.*;[10] (royal diamonds) Olson *et al.*;[9] (wine triangles) Bayfield *et al.*;[8] (orange squares) Hvelplund *et al.*[11]

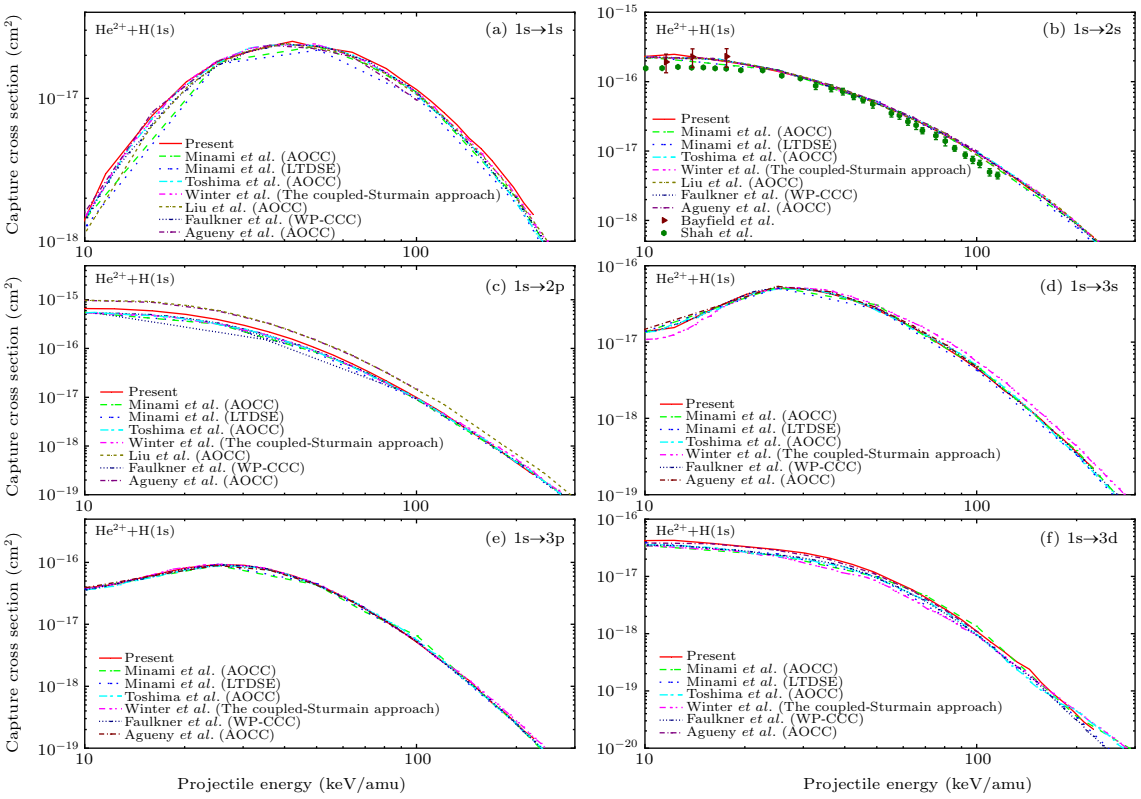


Fig. 4. The partial cross sections for electron captured into the 1s, 2*l* and 3*l* states of He^+ ions in He^{2+}–H(1s) collision. Theory: (solid red line) present results; (dashed green line) AOCC and (dotted blue line) LTDSE results of Minami *et al.*;[19] (dash-dotted cyan line) AOCC results of Toshima *et al.*;[15] (dash-dot-dotted magenta line) coupled-Sturmain approach results of Winter *et al.*;[18] (short dashed dark yellow line) AOCC results of Liu *et al.*;[16] (short dotted navy line) WP-CCC results of Faulkner *et al.*;[20] (short dash dotted purple line) AOCC results of Agueny *et al.*[17] Experiment: (wine triangles) Bayfield *et al.*;[8] (olive hexagons) Shah *et al.*[10]

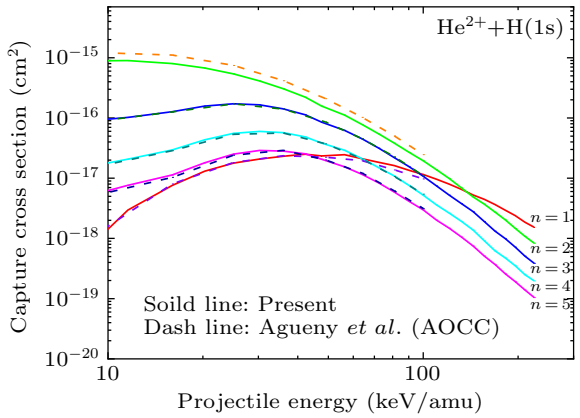


Fig. 5. The cross sections for electron captured into the $n = 1$–5 shells of He^+ ions in He^{2+}–H(1s) collision. The present results are denoted by solid lines; the results of Agueny *et al.*[17] are dashed lines.

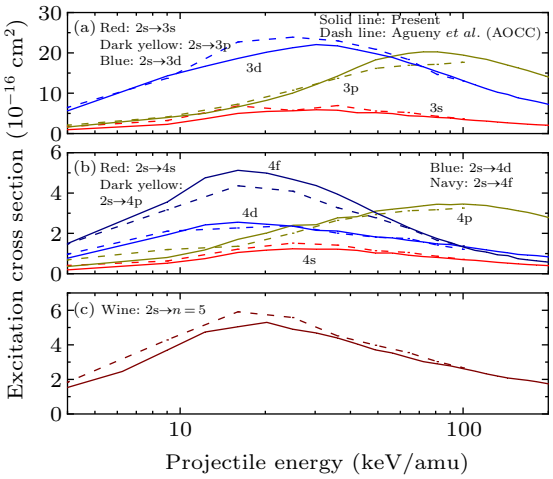


Fig. 6. Cross sections for excitation to $3l$, $4l$ and $n = 5$ channels of H atoms in He^{2+}–H(2s) collision. The present results are shown by solid lines; the results of Agueny *et al.*[17] are presented by dashed lines.

3.2. He^{2+}–H(2s) collision

3.2.1. Excitation cross sections

The research on the excitation process in collisions of He^{2+} with H(2s) atoms has been very limited. In Fig. 6(a), the cross sections for excitation to H($3l$) states in this collision are presented and compared with the results of Agueny *et al.*[17] For this collision system, H(2s) → H(3d) transition dominates for collision energies below 60 keV/amu. When the collision energy exceeds 60 keV/amu, the main channel becomes the 2s → 3p transition. It can be seen from this figure that our results are significantly different from those of Agueny *et al.*[17] in the regions near the peak of cross sections. The cross sections for excitation to the H($4l$) states of H atoms are shown in Fig. 6(b). The calculations from Agueny *et al.*[17] are also given in the same figure for comparison. It can be seen that the cross sections excitation to H($4l$) states are one order of magnitude smaller than those of the H($3l$) states. The present results have similar energy behavior with the results of Agueny *et al.*[17] in the entire energy region, but the magnitudes have slight differences. Simultaneously, the results of excitation to $n = 5$ channel are also displayed in Fig. 6(c) with the results of Agueny *et al.*[17] For the collision energy below 30 keV/amu, our results are smaller than Agueny's.[17] The reason for these discrepancies may be from the fact that a large size of AO expansion basis including pseudostates is used in the present AOCC method.

3.2.2. Electron capture cross sections

In Fig. 7, we present our total electron capture cross sections for He^{2+}–H(2s) collision and compare them with the results of the previous AOCC method of Esry *et al.*,[23] CTMC method of Blanco *et al.*,[21] and the MOCC method of Blanco *et al.*[21] and Jouin *et al.*[22] It is noted that in the energy region below 3 keV/amu, our results are slightly larger than those of MOCC method of Blanco *et al.*[21] and Jouin *et al.*,[22] and the AOCC results of Esry *et al.*[23] The reason for this difference is mainly from the fact that the expansion basis sets used in the previous calculations are too small. In the energy region of 3 keV/amu–10 keV/amu, the present result is in good agreement with the MOCC results of Jouin *et al.*[22] which used a 19-state basis set and the CTMC results of Blanco *et al.*[21] In the 10 keV/amu–30 keV/amu range, our results are consistent with the EI results of Montanari *et al.*[25] In the high energy region near 100 keV/amu, our results reproduce the results[24] of CDW and EI methods.

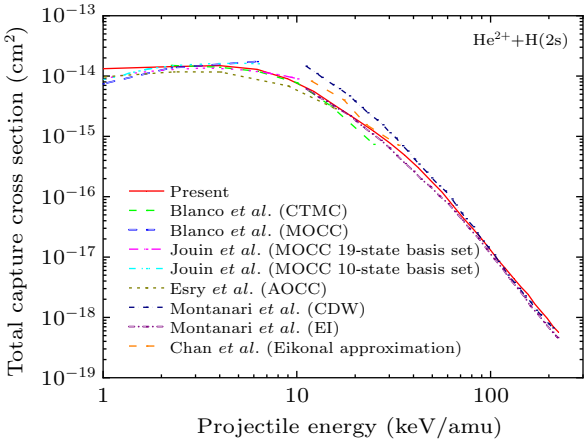


Fig. 7. The total electron capture cross sections as a function of energy in He^{2+}–H(2s) collision. Present results: solid red line; results of Blanco *et al.*:[21] dashed green line and double dashed blue line; results of Jouin *et al.*:[22] dash-dotted magenta line and dash-dot-dotted cyan line; results of Esry *et al.*:[23] short dashed dark yellow line; results of Montanari *et al.*:[25] short dash-dotted navy line and double short dash-dotted purple line; results of Chan *et al.*:[24] dashed orange line.

The partial cross sections for capture to the $3l$, $4l$ and $n = 4$, 5 channels of He^+ ions for this collision system are shown in Figs. 8(a)–8(d), 9(a)–9(d), and 10, respectively, and the other available theoretical results[17,21–23,25] are also provided for comparison. From these figures, we can see that

our results are all in good agreement with those of Agueny *et al.*[17] in the considered energy region, except for the 4f channel for the energies below 10 keV/amu. There are currently no experimental results reported for this system, so the differences between our calculations and other theoretical results in the figures need further study.

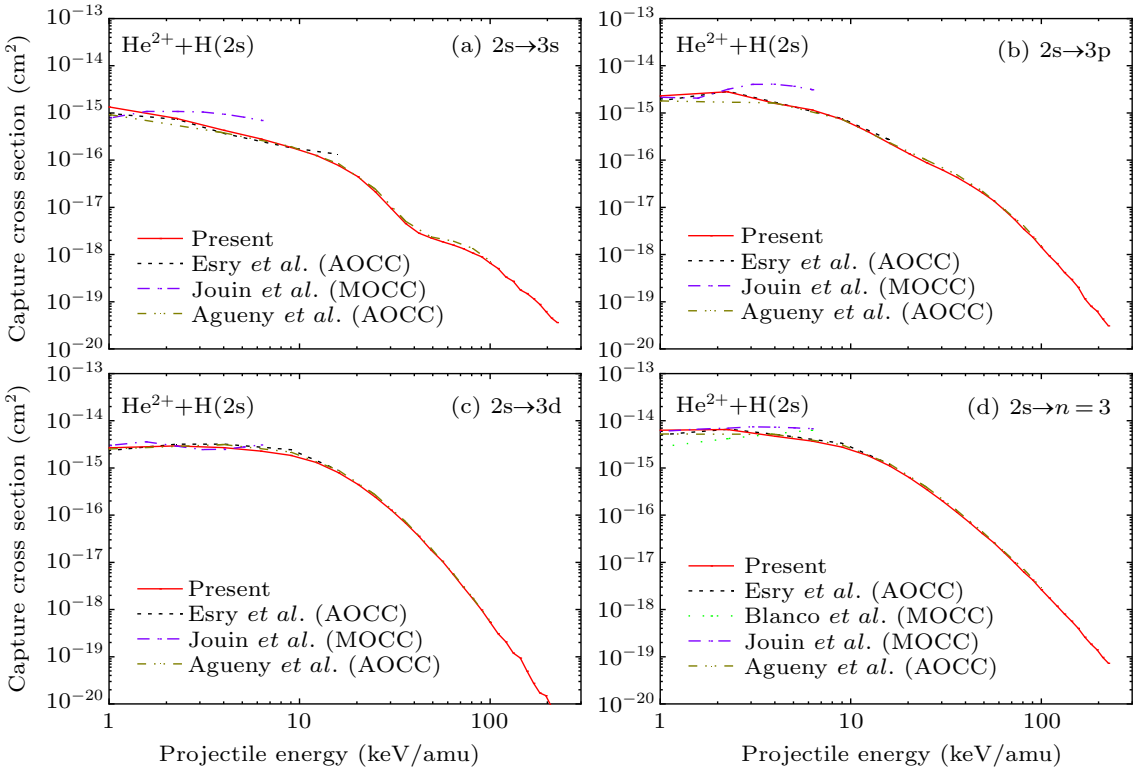


Fig. 8. The cross sections for electron captured into the $n = 3$ shell of He^+ ion in He^{2+}–H(2s) collision. Present results: solid red line; results of Esry *et al.*:[23] short dashed black line; results of Jouin *et al.*:[22] dash-dotted violet line; results of Agueny *et al.*:[17] dash-dot-dotted dark yellow line; results of Blanco *et al.*:[21] dotted green line.

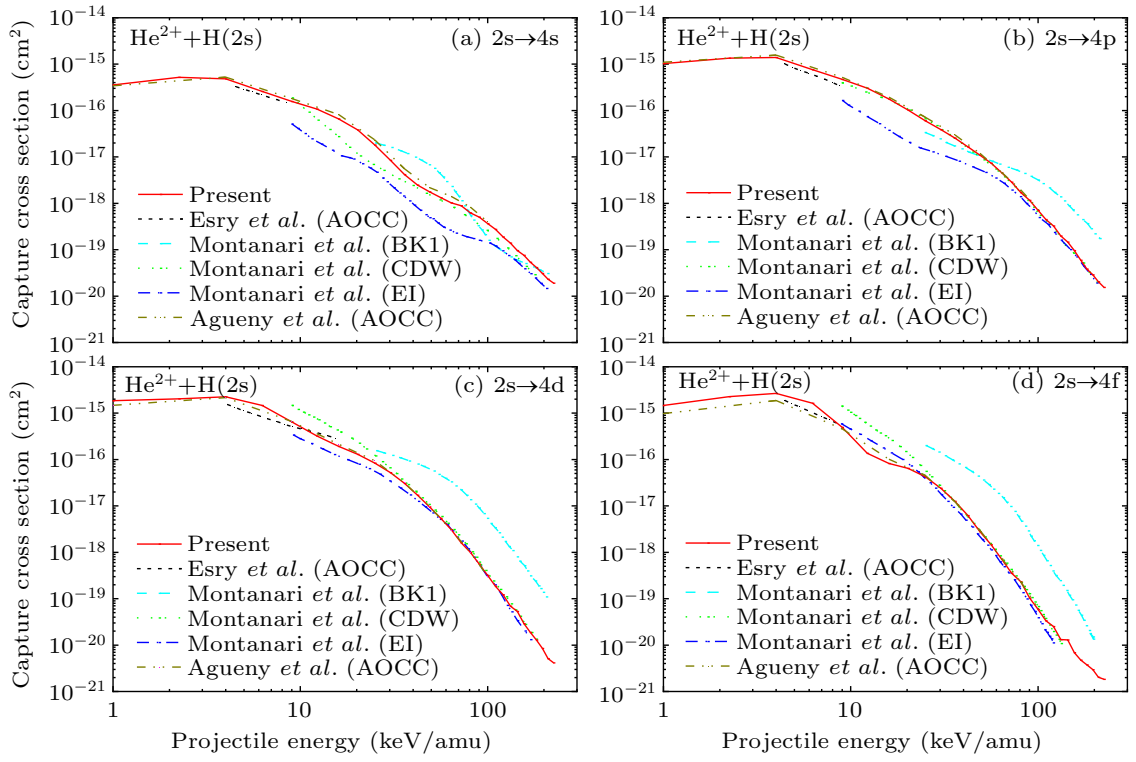


Fig. 9. The cross sections for electron captured into the $4l$ states of He^+ ions in He^{2+}–H(2s) collision. Present results: solid red line; results of Esry *et al.*:[23] short dashed black line; results of Montanari *et al.*:[25] dashed cyan line, dotted green line and blue dash dotted line; results of Agueny *et al.*:[17] dash-dot-dotted dark yellow line.

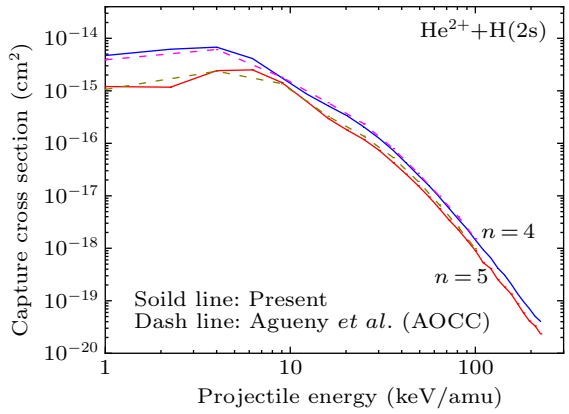


Fig. 10. The cross sections for electron captured into the $n = 4, 5$ shells of He^+ ions in He^{2+}–H(2s) collision. The present results are denoted by solid lines in different colors; the results of Agueny *et al.*[17] are dashed lines in different colors.

4. Conclusion

Using a semiclassical atomic orbital close-coupling approach, we have investigated the electron capture and excitation processes in He^{2+}–H(1s, 2s) collisions. The total and partial cross sections for these two processes have been reported in the energy region of 1 keV/amu–200 keV/amu, and compared with available theoretical and experimental data. It is found that the differences between the present results and the other theoretical results are mainly due to the fact that relatively large basis sets (especially the ionization channels represented by pseudostates) centered on the target and projectile are used in the present calculations. This can fully take into account the effect of multi-channel couplings for the collision process of these systems. Especially for the excitation process, the impact of the multi-channel couplings on the excitation cross sections can be clearly observed. In contrast, the cross sections for electron capture process are easier to converge, and the present results are consistent with those of the previous studies. The reliable cross sections from the present work are useful for the spectral simulation and diagonalization in astrophysics and laboratory plasma.

Data availability statement

The data that support the findings of this study are openly available in Science Data Bank at the following link https://doi.org/10.57760/sciencedb.j00113.00114

Acknowledgments

Project supported by the National Key Research and Development Program of China (Grant No. 2022YFA 1602500) and the National Natural Science Foundation of China (Grant Nos. 11934004 and 12241410).

References

[1] Anderson H, Hellermann M G von, Hoekstra R, Horton L D, Howman A C, Konig R W T, Martin R, Olson R E and Summers H P 2000 *Plasma Phys. Control. Fusion* **42** 781
[2] Delabie E, Brix M, Giroud C, Jaspers R J E, Marchuk O, O'Mullane M G, Ralchenko Y, Surrey E, Hellermann M G von, Zastrow K D and Contributors J E 2010 *Plasma Phys. Control. Fusion* **52** 125008
[3] Chluba J, Rubiño-Martín J A and Sunyaev R A 2007 *Monthly Notices of the Royal Astronomical Society* **374** 1310
[4] Shimoda J and Laming J M 2019 *Monthly Notices of the Royal Astronomical Society* **485** 5453
[5] Liu C L, Zou S Y, He B and Wang J G 2015 *Chin. Phys. B* **24** 093402
[6] Zhu X L, Cui S C, Xing D D, Xu J W, Najjari B, Zhao D M, Guo D L, Gao Y, Zhang R T, Su M G, Zhang S F and Ma X W 2024 *Chin. Phys. B* **33** 023401
[7] Gu L Y, Shah C and Zhang R T 2022 *Sensors* **22** 752
[8] Bayfield J E and Khayrallah G A 1975 *Phys. Rev. A* **12** 869
[9] Olson R E, Salop A, Phaneuf R A and Meyer F W 1977 *Phys. Rev. A* **16** 1867
[10] Shah M B and Gilbody H B 1978 *J. Phys. B: At. Mol. Phys.* **11** 121
[11] Hvelplund P and Andersen A 1982 *Phys. Scr.* **26** 375
[12] Hughes M P, Geddes J and Gilbody H B 1994 *J. Phys. B: At. Mol. Opt. Phys.* **27** 1143
[13] Detleffsen D, Anton M, Werner A and Schartner K H 1994 *J. Phys. B: At. Mol. Opt. Phys.* **27** 4195
[14] Fritsch W, Shingal R and Lin C D 1991 *Phys. Rev. A* **44** 5686
[15] Toshima N 1994 *Phys. Rev. A* **50** 3940
[16] Liu L, Wang J G and Janev R K 2008 *Phys. Rev. A* **77** 032709
[17] Agueny H, Hansen J P, Dubois A, Makhoute A, Taoutioui A and Sisourat N 2019 *Atomic Data and Nuclear Data Tables* **129–130** 101281
[18] Winter T G 2007 *Phys. Rev. A* **76** 062702
[19] Minami T, Lee T G, Pindzola M S and Schultz D R 2008 *J. Phys. B: At. Mol. Opt. Phys.* **41** 135201
[20] Faulkner J, Abdurakhmanov I B, Alladustov S U, Kadyrov A S and Bray I 2019 *Plasma Phys. Control. Fusion* **61** 095005
[21] Blanco S A, Falcon C A, Reinhold C O, Casaubon J I and Piacentini R D 1987 *J. Phys. B: Atom. Mol. Phys.* **20** 6295
[22] Jouin H and Harel C 1991 *J. Phys. B: At. Mol. Opt. Phys.* **24** 3219
[23] Esry B D, Chen Z, Lin C D and Piacentini R D 1993 *J. Phys. B: At. Mol. Opt. Phys.* **26** 1579
[24] Chan F T and Eichler J 1979 *J. Phys. B: Atom. Mol. Phys.* **12** L305
[25] Montanari C C, Gravielle M S and Miraglia J E 1997 *Phys. Scr.* **56** 279
[26] Ibaaz A, Hernandez R E, Dubois A and Sisourat N 2016 *J. Phys. B: At. Mol. Opt. Phys.* **49** 085202
[27] Pye C C and Mercer C J 2012 *J. Chem. Educ.* **89** 1405
[28] Kramida A, Ralchenko Y, Reader J and NIST ASD Team 2023 *NIST Atomic Spectra Database* (version 5.11).
[29] Gao J W, Miteva T, Wu Y, Wang J G, Dubois A and Sisourat N 2021 *Phys. Rev. A* **103** L030803